A Laminar Flow Electroporation System for Efficient DNA and siRNA Delivery

ARTICLE *in* ANALYTICAL CHEMISTRY · JUNE 2011

Impact Factor: 5.64 · DOI: 10.1021/ac200625b · Source: PubMed

10 AUTHORS, INCLUDING:

Xueming Li
Delft University of Technology
8 PUBLICATIONS **18** CITATIONS
SEE PROFILE

Huang Huang
Stanford University
10 PUBLICATIONS **145** CITATIONS
SEE PROFILE

Xiaoxia Wang
Peking University
19 PUBLICATIONS **80** CITATIONS
SEE PROFILE

Quan Du
Peking University
59 PUBLICATIONS **1,331** CITATIONS
SEE PROFILE

analytical chemistry

ARTICLE

pubs.acs.org/ac

A Laminar Flow Electroporation System for Efficient DNA and siRNA Delivery

Zewen Wei,[†,¶,§] Deyao Zhao,[‡,§] Xueming Li,[†] Mengxi Wu,[†] Wei Wang,[†] Huang Huang,[‡] Xiaoxia Wang,[‡] Quan Du,[*,‡] Zicai Liang,[*,‡] and Zhihong Li[*,†]

[†]National Key Laboratory of Science and Technology on Micro/Nano Fabrication, Institute of Microelectronics, Peking University, Beijing 100871, People's Republic of China

[¶]National Center for Nanoscience and Technology, Beijing 100190, People's Republic of China

[‡]Institute of Molecular Medicine, Peking University, Beijing 100871, People's Republic of China

Supporting Information

ABSTRACT: By introducing a hydrodynamic mechanism into a microfluidics-based electroporation system, we developed a novel laminar flow electroporation system with high performance. The laminar buffer flow implemented in the system separated the cell suspension flow from the electrodes, thereby excluding many unfavorable effects due to electrode reaction during electroporation, such as hydrolysis, bubble formation, pH change, and heating. Compared to conventional microfluidic electroporation systems, these improvements significantly enhanced transfection efficiency and cell viability. Furthermore, successful electrotransfection of plasmid DNA and, more importantly, synthetic siRNA, was demonstrated in several hard-to-transfect cell types using this system.

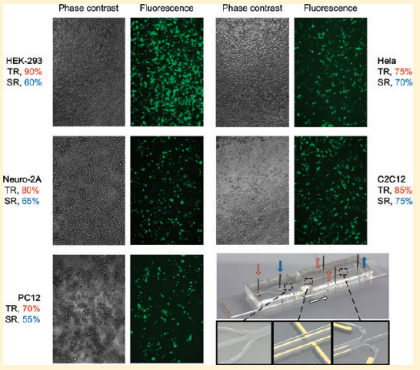

INTRODUCTION

Cell transfection is a basic technology in molecular biology. For many biomedical practices such as antibody production and gene therapy, large numbers of cells must be transfected with plasmid DNA and/or synthetic siRNA.[1,2] Flow-through microelectroporation systems were recently developed for this purpose to facilitate high-throughput electroporation of a large number of mammalian cells. Since the proof-of-concept of microfluidic electroporation in 2001,[3] a variety of modified strategies have exploited particular channel geometries,[4−6] mechanical valves,[7] microfluidic droplets,[8] polyelectrolytic salt bridges,[9] and hydrodynamic focusing[10] to improve performance, as well as to decrease the applied voltage needed for efficient gene delivery. More recently, complex electrode modifications[9] and AC electric field[11] were also used in microfluidic electroporation systems to decrease bubble generation. However, some of the inherent damaging effects of electroporation (for example, hydrolysis, bubble formation, and pH variation) have not been satisfactorily addressed. In addition, new problems such as shear stress arising from microfluidic systems significantly compromise performance. Even though acceptable transfection efficiency is achieved with a few easy-to-transfect cell types, together, these unfavorable effects contribute to the relatively low transfection efficiency and high mortality in many physiologically important cell types. Such drawbacks prevent existing technologies from becoming general practice in biomedical research.

In this study, a novel microfluidic electroporation system integrating liquid isolated electrodes into a conventional flow electroporation system was developed. The laminar buffer flow implemented in this design successfully separated the cell suspension flow from the electrodes, therefore avoiding many of the damaging effects due to electrode reactions. Using this device, we achieved efficient plasmid and siRNA delivery in many hard-to-transfect cells. Compared with conventional systems, much-higher transfection efficiency and better cell viability were achieved.

EXPERIMENTAL SECTION

Design and Fabrication of the Laminar Flow Electroporation System. The design and a prototype of the proposed laminar flow electroporation (LFE) system are shown in Figure 1. Distinct from conventional flow electroporation (CFE) systems,[3,12] the LFE system exploited triple-layer laminar flow in electroporation, thereby excluding many of the unfavorable side effects reported in previous studies.[11,13] From a functional point of view, the microfluidic channel fabricated in LFE systems is divided into three segments: concentration, electroporation, and collection. In the LFE system, the cell suspension was

Received: March 10, 2011
Accepted: June 17, 2011
Published: June 17, 2011

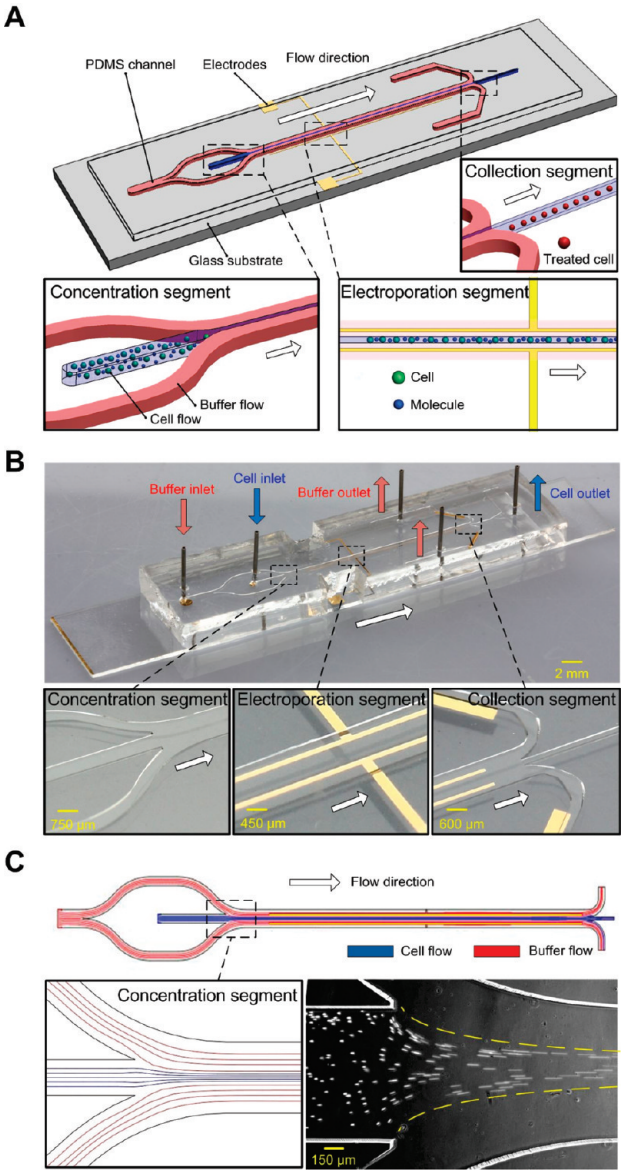

Figure 1. Design and prototype of laminar flow electroporation system: (A) schematic view of the LFE system and closeup of the three functional segments of the microfluidic channel; (B) prototype of the LFE system; and (C) simulated and microscopically recorded triple-layer flow implemented in the system.

delivered into the middle channel from the cell inlet and compressed into a thin layer in the concentration segment by the buffer coming from two side channels. The mixture flow, consisting of an inner cell suspension flow and two sheath buffer flows, then passed through the electroporation segment of the microchannel, in which two parallel Au electrodes placed on the sides of the channel produced a uniform electrical field distribution, which mediated gene electrotransfection. After electroporation, the cell suspension was separated from the sheath buffer flow and collected finally at the cell outlet, in the collection segment.

Fabrication of the laminar flow electroporation system was previously described[14] and is shown schematically in Supplementary Figure 1 in the Supporting Information. A precleaned 4-in. Pyrex7740 (Dow Corning, USA) glass wafer was used as the substrate, because it has high resistivity and transparency. Gold and chrome served as functional and adhesive materials for the microelectrodes, respectively. Gold is widely used in biological apparatus, because of its high conductivity, good chemical stability, and nontoxicity. The electrode was sputtered and patterned on the glass substrate by simple one-mask lithography and wet etch. The thicknesses of the gold layer and chrome layers were 300 and 30 nm, respectively. The microfluidic channel was fabricated with polydimethylsiloxane (PDMS, Dow Corning, USA), which is a transparent silicone material commonly used for the manufacture of microscale structures. A silicon master mold was fabricated via KOH etching. PDMS was cast into the master mold and heated to 70 °C for 1 h before it was peeled off and punched to create the inlet and outlet holes. After dicing to proper size and treatment by oxygen plasma in a plasma cleaner (CAS Instruments, PRC), the PDMS chip and the glass/electrode substrate were aligned and bonded, and then they were baked at 120 °C for 1 h to achieve strong bonding. A prototype of the microfluidic electroporation system is shown in Figure 1B. The two electrodes were 25 mm long, 100 μm wide, and spaced 500 μm apart. The electroporation channel was 30 mm long, 1.2 mm wide, and 50 μm high.

Electroporation Procedures. In electroporation, the two inlets of the device were connected to a syringe pump (Lange Instruments, PRC), and the two electrodes were wired to a pulse generator (BTX Apparatus, USA). Cultured cells were harvested by trypsin treatment and resuspended to a density of 1×10^4 cells/μL in a modified hypo-osmolar buffer (25 mM KCl, 0.3 mM KH_2PO_4, 0.85 mM K_2HPO_4, 36 mM myo-inositol, pH 7.2, conductivity 3.5 mS/cm at 25 °C). Plasmid DNA or siRNA was added to a final concentration of 20 μg/mL or 6 pmol/μL, respectively. The cells and molecules to be electroporated were delivered to the microfluidic channel through the cell inlet, and buffer solution was pumped into the channel through the buffer inlet. Electrical pulses were applied to the cells passing between the electrodes. The amplitude, duration, and interval of the electrical pulses were optimized for efficient gene delivery in different cell types. After electroporation, the cell suspension collected at the cell outlet was transferred into a 96-well cell culture plate, and a 200-μL normal culture medium was immediately added into each well. Twenty-four hours (24 h) later, the number of GFP-expressing cells was counted in five randomly chosen fields, using ImageJ from NIH, under a fluorescence microscope (Olympus). The fluorescence threshold for GFP-expressing cells was manual determined by visually check the transfected cells. Surviving cells were assessed by the propidium iodide exclusion assay. For each transfection, efficiency was calculated by dividing the number of GFP-expressing cells by the number of living cells, while the viability ratio was obtained by comparing the numbers of living cells in treated and untreated samples. Presented data are the average of three independent assays.

Oligonucleotides, Plasmids, and Cell Culture. DNA oligonucleotides from Invitrogen (Beijing, PRC) were used for vector construction and quantitative RT-PCR, and siRNA oligonucleotides were from Ribobio (Guangzhou, PRC). The oligonucleotide sequences are presented in Supplementary Data S1 in the Supporting Information.

The transfection efficiency of plasmid DNA was determined by pEGFP-C3 plasmid encoding an enhanced green fluorescent protein (Clontech). Purification of plasmid DNA was performed using an EndoFree Plasmid Maxi Kit (Qiagen, Germany).

HEK-293A, Hela, neuro-2A, and HEK-293 cells were grown in Dulbecco's modified Eagle's medium (DMEM) supplemented with 10% fetal bovine serum (Hyclone), 100 units/mL penicillin and 100 μg/mL streptomycin (Life Technologies, Gibco). PC-12 cells were grown in DMEM supplemented with 10% horse serum (Gibco) and 5% FBS. Cells were maintained at 37 °C in a 5% CO_2 humidified incubator.

RNAi Assay. Human embryonic kidney cells (HEK293) were grown in DMEM supplemented with 10% fetal bovine serum, 2 mM L-glutamine, 100 units/mL penicillin, and 100 μg/mL streptomycin (Life Technologies, Gibco). The cells were seeded into 24-well plates at a density of ~1×10^5 cells/well one day before transfection. A siQuant vector of 0.17 μg/well carrying the target site of tested siRNA was transfected into the cells at ~50% confluence, together with pRL-TK control vector at 0.017 μg/well, with or without 13 nM siRNA. The activity of both luciferases was determined by a fluorometer (Synergy HT, BioTek, USA) before the firefly luciferase activity was normalized to the renilla luciferase for each well. The silencing efficiency of each siRNA was calculated by comparison with a sample without siRNA treatment. All experiments were performed in triplicate and repeated at least twice.

Quantitative RT-PCR. Quantitative RT-PCR was performed using the Mastercycler ep realplex (Eppendorf) in combination with SYBR Green (Roche Applied Science, Mannheim, Germany). Briefly, total RNA was extracted using Trizol reagent (Invitrogen). RNA (2 μg) was reverse-transcribed to first-strand cDNA using oligo(dT) primer and an ImProm-II Reverse Transcriptase kit (Promega). The PCR profile was as follows: 95 °C for 30 s and 35 cycles at 95 °C for 30 s, 61 °C for 30 s, and 72 °C for 30 s. The amount of SYBR Green was measured at the end of each cycle. The cycle number at which the emission intensity of the sample rose above baseline was referred to as the threshold cycle and was proportional to the target concentration. Presented data are the average of three independent assays.

RESULTS AND DISCUSSION

The introduction of microfluidics into electroporation has made batch processing of large numbers of mammalian cells easier and more cost-effective. However, some problems in current designs remain to be solved. Water electrolysis due to electrode reaction presents a major challenge in practice, resulting in bubble formation, heating, and dramatic pH change. Our preliminary data also demonstrated that these effects, together, compromise cell transfection efficiency and viability (see Supplementary Figure 2 in the Supporting Information).

A Laminar Flow Electroporation System. To overcome these damaging effects, we developed a novel microfluidic electroporation system. Shown schematically in Figure 1A, this system consisted of a glass substrate with a microfabricated electrode pair and a mounted silicon matrix with a microfluidic electroporation channel. The cell suspension pumped into the channel through the cell inlet was compressed into a middle flow by the sheath buffer flows from the two buffer inlets. Therefore, the cells to be electroporated were separated from the electrodes, reducing the many unfavorable effects caused by electrode reaction during electroporation. To increase the processing capacity, as well as to avoid channel blockage by cell aggregation, a relatively large electroporation channel 30 mm long, 1.2 mm wide, and 50 μm high was fabricated. A parallel Au electrode pair was placed inside the microchannel to deliver uniform electrical

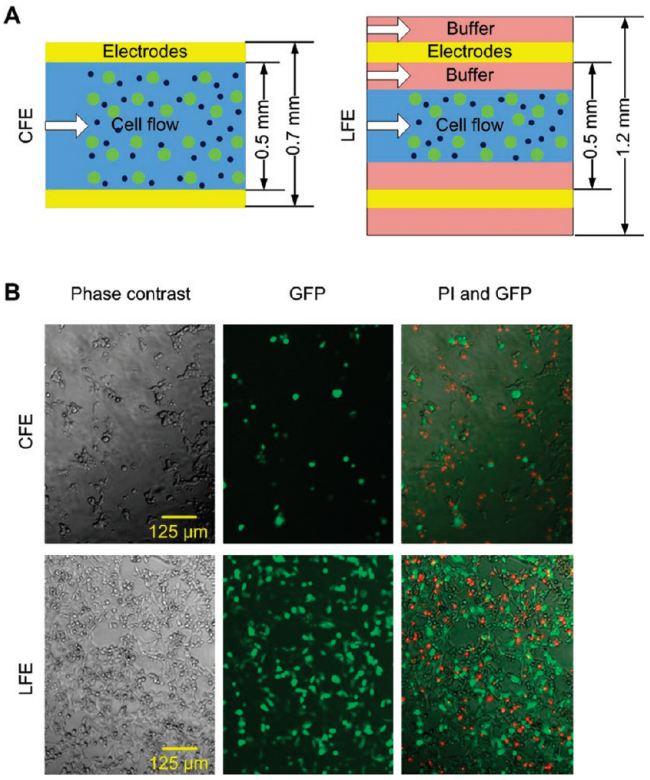

Figure 2. (A) Configurations of CFE and LFE systems (green dots represent cells to be transfected; black dots represent molecules to be delivered). (B) Performance of CFE and LFE systems. Using these two microfluidic electroporation systems, cultured HEK-293 cells were transfected by GFP-expression plasmid. Twenty-four hours after electroporation, transfection efficiency and cell viability were assessed by GFP expression under a fluorescence microscope and PI exclusion.

pulses (see Supplementary Figure 3 in the Supporting Information) to cells passing between them, mediating efficient gene transfection. As shown in Figure 1C, the numerical analysis of cell traces by Comsol 3.5a (COMSOL AB, USA), as well as microscopic observation, indicated that cells passed through the electroporation segment in the middle flow, which was shielded from the electrodes by the two lateral sheath flows.

To determine whether the novel design did improve performance, a laminar flow electroporation device (LFE; see Figures 1B and 2A) and a conventional flow electroporation device (CFE; see Figure 2A and Supplementary Figure 4 in the Supporting Information) were fabricated and tested. For the purposes of comparison, the two devices were similarly designed and fabricated in terms of the physical properties of the electrodes and the channel. In addition, a constant cell suspension flow rate of 20 μL/min, and rectangular electric pulses of 70 V and 0.1 ms duration, were applied in the electroporation. Using the CFE and LFE devices, HEK-293 cells were electroporated with a green fluorescent protein-expressing plasmid (pEGFP-C3). Ninety percent (90%) transfection efficiency and 60% cell viability were demonstrated with the LFE device, which were significantly higher than those with the CFE device (see Figures 2B and 3A).

To further understand the improvement from the CFE system to the LFE system, the effects of increasing the pulse strength on transfection efficiency and cell viability were investigated (see Figure 3A). In the LFE system, increasing the pulse voltage from

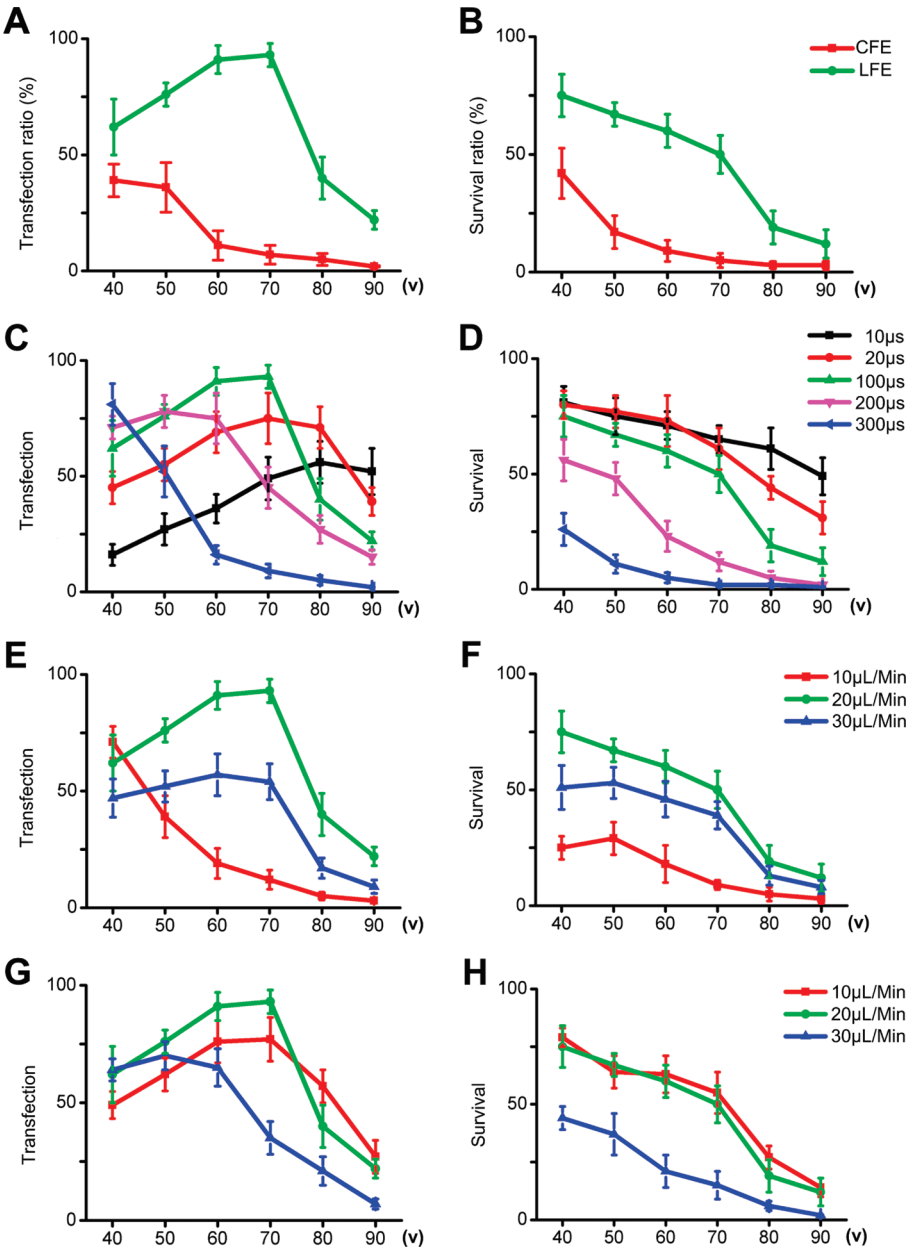

Figure 3. Optimization of electroporation parameters. To evaluate the effects of electroporation parameters on cell transfection and viability, GFP-expression plasmid was transfected into cultured HEK-293 cells. Transfection efficiency and cell viability were assessed by GFP expression and PI exclusion after 24 h. The number of GFP-expressing cells was counted in five randomly chosen fields; the number of living cells was determined by PI exclusion. The transfection rate (TR) is estimated by the number of transfected cells versus living cells; the survival rate (SR) is estimated by the number of living cells in treated and untreated samples. (A,B) Transfection efficiency and cell viability as a function of pulse voltage in different system configurations. (C,D) Transfection efficiency and cell viability as a function of pulse duration, when pulse interval was 2 s. (E,F) Transfection efficiency and cell viability as a function of flow velocity, when pulse interval was 2 s. (G,H) Transfection efficiency and cell viability as a function of flow velocity. To maintain a fixed number of pulses, the pulse frequency was adjusted according to cell flow rate. Data were presented as the mean ± the standard deviation (SD), $n = 6$.

40 V to 70 V resulted in a significant gain of transfection, while a further increase from 70 V to 90 V compromised transfection. With a much lower transfection efficiency, a similar profile of transfection versus voltage was observed for the CFE system. In addition to the improvement in transfection efficiency, a remarkable inverse correlation was found between cell viability and pulse strength, for both the CFE and LFE systems (Figure 3B). Longer exposure to pulses greatly compromised cell viability. At the same pulse voltage, significantly higher cell viability was obtained in the LFE system than in the CFE system. As expected, these results demonstrated that isolating the cell suspension from the electrodes greatly improved the performance of the microfluidic electroporation system.

Optimization of Electroporation Parameters. In contrast to a previously reported chip-based electroporation device,[15] a prominent feature of microfluidic electroporation systems is that they provide a cost-effective solution for the transfection of large volumes of cells. To optimize the performance of this device, the

dx.doi.org/10.1021/ac200625b |*Anal. Chem.* 2011, 83, 5881–5887

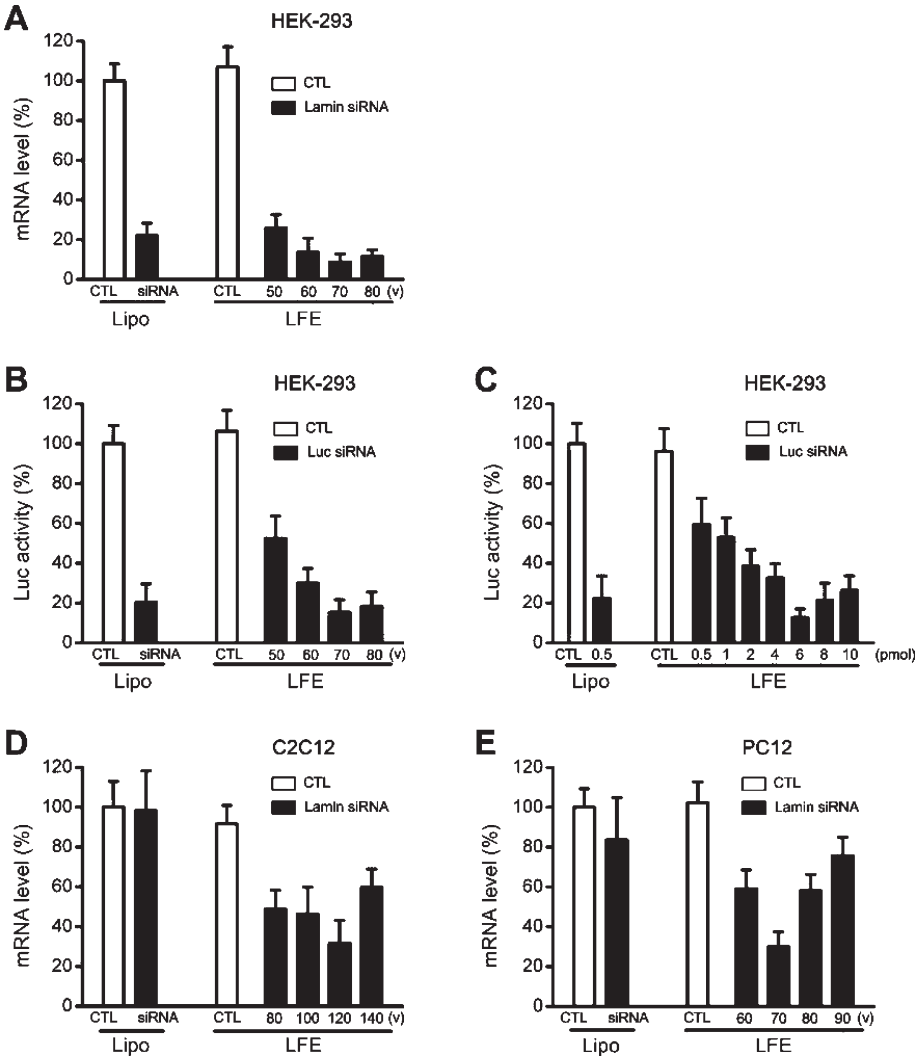

Figure 4. Electrotransfection of synthetic siRNA mediates potent gene silencing. (A) Lamin A/C-targeting siRNA was transfected into HEK-293 cells by Lipofectamine 2000, and the LFE system with different pulse voltages. (B,C) Cotransfection of a luciferase-expressing vector and a luciferase-targeting siRNA was performed in HEK-293 cells, using Lipofectamine 2000 and the LFE system. Effects of pulse voltage (B) and siRNA concentration were assessed in terms of silencing efficiency. (D) Synthetic siRNA targeting Lamin A/C was transfected into C2C12 cells by Lipofectamine 2000 and the LFE system. Gene silencing at the protein level was measured by dual-luciferase assay, and gene silencing at the mRNA level was assessed by quantitative RT-PCR. Data were presented as the mean ± the standard deviation (SD), $n = 6$.

effects of varying pulse voltage and duration, as well as cell flow rate, were determined, in terms of cell transfection and viability. From our previous chip electroporation study, buffer ionic strength and osmolarity are also important parameters determining cell viability in electroporation; therefore, a buffer ionic strength of 25 mM and an osmolarity of 90 mOsm/L were used in the subsequent assays. To maintain a constant distance (~100 μm) between cell suspension and electrodes, the velocity ratio between cell suspension and buffer flow was maintained at 1:3 for all experiments performed in the study (velocity of cell flow, 20 μL/min; buffer sheath flow, 60 μL/min). Figure 3C and 3D shows the influence of pulse duration on transfection and viability. The longer the pulse duration, the lower the voltage needed to achieve optimal cell transfection. On the other hand, cell viability decreased steadily with voltage, since stronger electric fields presumably cause more damage to the cell membrane.

We then investigated the effects of flow velocity on cell transfection and viability, in which the pulse conditions were set at 70 V and 0.1 ms and pulse interval of 2 s (see Figures 3E and 3F). Compared to electroporation at a flow velocity of 20 μL/min, double electric pulses were exerted on passing cells in electroporation at a flow velocity of 10 μL/min. This double treatment resulted in extensive cell death and significantly compromised cell transfection efficiency. When the flow velocity was set at 30 μL/min, transfection improved; however, the strong shear force due to the rapid movement caused cell lysis. Taken together, these experiments indicated that flow velocity and pulse frequency were crucial factors in this microfluidics-based electroporation system.

To differentiate the role of flow velocity from pulse number, additional experiments were carried out (see Figures 3G and 3H). To keep the pulse number acting on each passing cell unchanged at different flow velocities, the pulse frequency was adjusted accordingly. The results demonstrated consistent profiles of transfection efficiency versus voltage at different flow velocity settings. Nevertheless, the highest mortality occurred at 30 μL/min, which indicated the role of shear force in this scenario.

dx.doi.org/10.1021/ac200625b |*Anal. Chem.* 2011, 83, 5881–5887

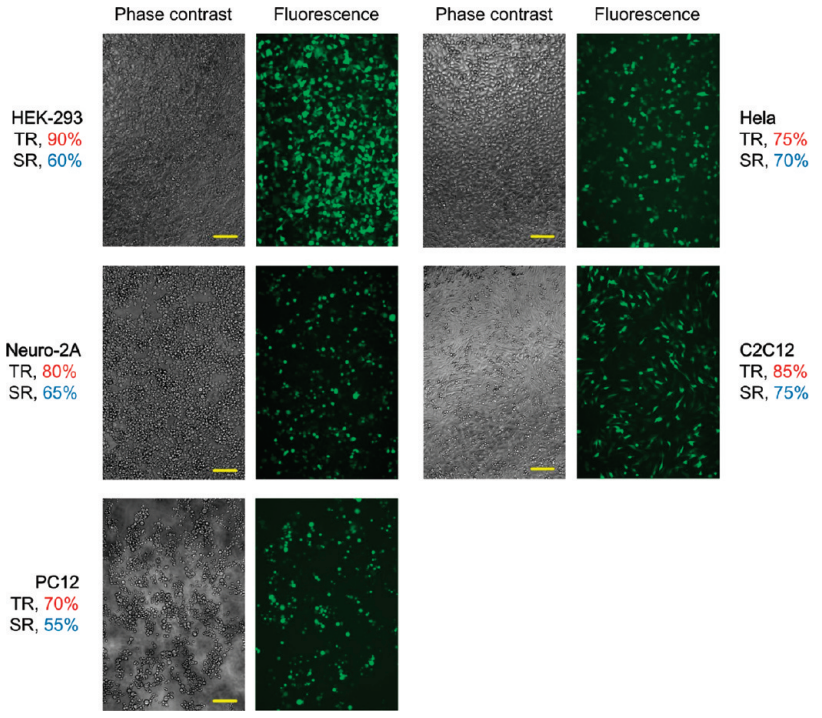

Figure 5. A universal plasmid DNA delivery platform. Using the LFE system, pEGFP plasmid was transfected into different cultured cells. Twenty-four hours (24 h) after electroporation, the number of GFP-expressing cells was counted in five randomly chosen fields; the number of living cells was determined by PI exclusion. The transfection rate (TR) was estimated by the number of transfected cells versus living cells; the survival rate (SR) was estimated by the number of living cells in treated and untreated samples. Optimized electroporation parameters: HEK-293 cells, pulse strength 70 V and duration 0.1 ms; Hela cells, 60 V and 0.1 ms; Neuro-2A cells, 90 V and 0.1 ms; C2C12 cells, 120 V and 0.1 ms; PC-12 cells, 70 V and 0.1 ms. Other common parameters: cell flow rate, 20 μL/min; sheath buffer flow rate, 60 μL/min; pulse interval, 2 s; scale bar, 400 μm.

Electrotransfection of Synthetic siRNA. RNAi has become an important technology for manipulating cellular phenotypes, understanding gene functions, and discovering novel therapeutic targets.[16,17] However, because of the large size and high adverse charge, siRNA delivery remains problematic. To the best of our knowledge, no successful siRNA delivery has been reported in microfluidic electroporation systems. To determine the utility of the LFE system in siRNA delivery, a Lamin A/C siRNA was first electroporated into easy-to-transfect HEK-293 cells. For comparison, Lipofectamine 2000 transfection[15,18] was included in the experiments as a control. Twenty-four hours (24 h) after electroporation, the expression levels of Lamin-AC were assessed by quantitative RT-PCR (Figure 4A). As expected, 78% of target gene knockdown was mediated by Lipofectamine transfection. With electroporation, similar and even better gene silencing efficiency was obtained; notably, a correlation between pulse voltage and gene silencing was found, with the highest silencing level being 92% (see Figure 4A). Furthermore, cotransfection of plasmid DNA and synthetic siRNA was performed in HEK-293 cells. To facilitate quantitatively measurement of gene silencing activity, an active siRNA targeting firefly luciferase was electroporated into the cells, together with a luciferase-expressing plasmid. The resulting gene-silencing in protein was determined by dual-luciferase assay. Significant target gene repression demonstrated simultaneous delivery of both plasmid DNA and siRNA (see Figures 4B and 4C). The results further revealed a dose-dependent gene silencing effect (see Figure 4C). Interestingly, a clear correlation between pulse voltage and gene silencing effect was revealed for both mRNA (Figure 4A) and protein (Figure 4B) levels in HEK-293 cells, showing that a pulse voltage of 70 V resulted in optimal gene silencing. While a lower pulse voltage was not enough for efficient gene transfection in HEK-293 cells, pulse voltages higher than 70 V resulted in serious cell mortality, which also translated into low delivery efficiency.

Next, we targeted the difficult-to-transfect cell types for siRNA delivery, C2C12 and PC12 (see Figures 4D and 4E). Lamin A/C siRNA was electroporated into these cells as previously described. In C2C12 cells, 68% gene knockdown was achieved by LFE electroporation, while transfection by Lipofectamine did not show any silencing effects. However, in PC12 cells, gene-silencing efficiency as high as 70% was obtained by LFE electroporation, which was much higher than that by Lipofectamine transfection (20%). Furthermore, extensive cytotoxicity was observed in Lipofectamine transfection.

Electrotransfection of Plasmid DNA. To evaluate the flexibility of the LFE system in plasmid DNA transfection, pEGFP plasmid was electroporated into a range of cell types representing different levels of difficulty in gene delivery. In contrast to easy-to-transfect HEK-293 cells, we included Hela cells derived from a cervical adenocarcinoma, which are known to be difficult to transfect by chemical approaches such as Lipofectamine 2000. Other cell types in the assay included the folllowing: Neuro-2A cells, a neuroblastoma cell line; PC-12 cells, a pheochromocytoma cell line derived from rat adrenal medulla and often used in neuronal differentiation studies; and undifferentiated C2C12 cells. C2C12 is a mouse myoblast cell line established by Yaffe and Saxel in 1977, which undergoes rapid differentiation *in vitro*, forms contractile myotubes, and produces characteristic muscle proteins. C2C12 and PC12 cells are refractory to Lipofectamine 2000 transfection, and even with conventional microfluidic electropora-

tion systems, successful transfection of C1C12 and PC12 cells has never been reported.

With high degrees of transfection and low cell mortality, we successfully transfected these physiologically important cell lines. For comparison purposes, a cell flow velocity of 20 μL/min and a buffer flow rate of 60 μL/min were used. The pulse parameters were individually optimized for a balance between transfection efficiency and cell viability. Twenty-four hours (24 h) after treatment, EGFP expression was visually checked for transfected cells and PI exclusion staining was performed to visualize the dead cells. In comparison with published studies, higher transfection efficiency and viability were obtained, depending on the cell type (see Figure 5). Particularly in C2C12 cells, which are known to be refractory to most current transfection strategies, a transfection efficiency of 85% and a cell viability of 75% were achieved. Taken together, the optimal and consistent transfection indicates that the LFE system mediated efficient gene delivery in extensive cell populations without cytotoxicity.

To further validate this system, a prolonged test was performed continuously over the course of 3 h. Analysis of randomly sampled cells showed consistent cell transfection efficiency and viability, demonstrating that this system can stably function over a long time course.

CONCLUSION

In the present study, we demonstrated a laminar flow electroporation system by implementing liquid isolated electrodes in a conventional microfluidic electroporation system. By introducing triple-layer laminar flow, the cell suspension was separated from the electrodes in electroporation, thereby avoiding many harmful effects, such as bubble formation, heating, and dramatic pH changes caused by hydrolysis, predominantly at the cathode. Well-designed channel size and flow velocity prevent cells from being damaged by shear force. These improvements translated into high cell transfection efficiency and viability in practice. As proof of concept, several difficult-to-transfect cell lines were successfully electrotransfected by the LFE system, using both plasmid DNA and siRNA. Furthermore, another clear advantage of this system is that large numbers of cells can be processed in a given time, providing many opportunities for novel applications in DNA and siRNA delivery.

ASSOCIATED CONTENT

Supporting Information. *Supplementary Data S1* is a table giving information about DNA and RNA oligonucleotides. *Supplementary Data S2* is a table showing a comparison of microfluidic electroporation devices. *Supplementary Figure 1* shows a fabrication of microfluidic electroporation system. PDMS channel was fabricated by soft lithography, electrodes were fabricated on a glass substrate by one-mask lithography and wet etch. *Supplementary Figure 2* shows bubble formation and pH variance in electroporation. ((A) Bubbles were slightly generated near cathode, under electric pulses with 60 V in amplitude, 0,1 ms in pulse duration. Cell flow channel was outlined by white arrow line. (B) Higher voltage (90 V) and longer pulse duration (0.2 ms) accelerate bubble generation. (C) Continuously enhanced bubble generation. Voltage is 140 V and pulse duration is 0.3 ms. (D) pH value change (purple area near cathode) was observed.) Electrical condition is 140 V and 0.3 ms. Bubble formation was monitored by microscopy (Nikon, Japan), and pH variance change was monitored by a pH indicator phenolphthalein. *Supplementary Figure 3* shows the simulated electrical field distribution in LEF system (Comsol 3.5a, COMSOL AB, USA). Voltage is 80 V. *Supplementary Figure 4* is a photograph of a fabricated conventional flow electroporation chip. This information Is available free of charge via the Internet at http://pubs.acs.org/

AUTHOR INFORMATION

Corresponding Author

*Faxes: +86-10-62750799 (Q.D.), +86-10-62769862 (Z. Liang), +86-10-62751789 (Z. Li). E-mail addresses: quan.du@pku.edu.cn (Q.D.), liangz@pku.edu.cn (Z. Liang), and zhhli@ime.pku.edu.cn (Z. Li).

Author Contributions

§These authors contributed equally to the work.

ACKNOWLEDGMENT

This work was supported by the National High-tech R&D Program of China (No. 2007AA02Z165), the National Basic Research Program of China (Nos. 2011CBA01100 and 2007CB512100), the National Drug Program (No. 2009ZX09503), the National Natural Science Foundation of China (Nos. 60976086, 30873187, and 30871385), and the Beijing Natural Science Foundation (No. 5092011). We thank Dr. I. C. Bruce for critically reading this manuscript.

REFERENCES

(1) Goodnow, C. C.; Vinuesa, C. G.; Randall, K. L.; Mackay, F; Brink, R. *Nat. Immunol.* **2010**, *11*, 681–688.
(2) Dove, A. *Nat. Methods* **2009**, *6*, 851–856.
(3) Lin, Y. C.; Jen, C. M.; Huang, M. Y.; Wu, C. Y.; Lin, X. Z. *Sens. Actuators: B* **2001**, *79*, 137–143.
(4) Shin, Y. S.; Cho, K.; Kim, J. K.; Lim, S. H.; Park, C. H.; Lee, K. B.; Park, Y.; Chung, C.; Han, D. C.; Chang, J. K. *Anal. Chem.* **2004**, *76*, 7045–7052.
(5) Kim, J. A.; Cho, K.; Shin, Y. S.; Jung, N.; Chung, C.; Chang, J. K. *Biosens. Bioelectron.* **2007**, *22*, 3273–3277.
(6) Geng, T.; Zhan, Y.; Wang, H. Y.; Witting, S. R.; Cornetta, K. G.; Lu, C. *J. Controlled Release* **2010**, *144*, 91–100.
(7) Wang, J.; Stine, M. J.; Lu, C. *Anal. Chem.* **2007**, *79*, 9584–9587.
(8) Zhan, Y.; Wang, J.; Bao, N.; Lu, C. *Anal. Chem.* **2009**, *81*, 2027–2031.
(9) Kim, S. K.; Kim, J. H.; Kim, K. P.; Chung, T. D. *Anal. Chem.* **2007**, *79*, 7761–7766.
(10) Zhu, T.; Luo, C.; Huang, J.; Xiong, C.; Ouyang, Q.; Fang, J. *Biomed. Microdevices* **2010**, *12*, 35–40.
(11) Ziv, R.; Steinhardt, Y.; Pelled, G.; Gazit, D.; Rubinsky, B. *Biomed. Microdevices* **2009**, *11*, 95–101.
(12) Li, L. H.; Shivakumar, R.; Feller, S.; Allen, C.; Weiss, J. M.; Dzekunov, S.; Singh, V.; Holaday, J.; Fratantoni, J.; Liu, L. N. *Technol. Cancer Res. Treat.* **2002**, *1*, 341–350.
(13) Wang, S.; Zhang, X.; Wang, W.; Lee, L. J. *Anal. Chem.* **2009**, *81*, 4414–4421.
(14) Wei, Z.; Huang, H.; Wu, M.; Liang, Z.; Wang, W.; Li, Z. In *Proceedings of MicroTAS*, 2010; pp 1622−1624 (Paper No. W58A).
(15) Huang, H.; Wei, Z.; Huang, Y.; Zhao, D.; Zheng, L.; Cai, T.; Wu, M.; Wang, W.; Ding, X.; Zhou, Z. *Lab Chip* **2010**, *11*, 163–172.
(16) Brooks, T. A.; Hurley, L. H. *Nat. Rev. Cancer* **2009**, *9*, 849–861.
(17) Eguchi, A.; Meade, B. R.; Chang, Y. C.; Fredrickson, C. T.; Willert, K.; Puri, N.; Dowdy, S. F. *Nat. Biotechnol.* **2009**, *27*, 567–571.
(18) Alvarez-Erviti, L.; Seow, Y.; Yin, H. F.; Betts, C.; Lakhal, S.; Wood, M. J. A. *Nat. Biotechnol.* **2011**, *29*, 341–345.